Polymer Testing 124 (2023) 108068

Contents lists available at ScienceDirect

Polymer Testing

journal homepage: www.elsevier.com/locate/polytest

Mechanical, electrical, and adhesive synergies in melt-processed hybrid bio-based TPU nanocomposites

N. Aranburu, I. Otaegi, G. Guerrica-Echevarria *

POLYMAT and Department of Advanced Polymers and Materials: Physics, Chemistry and Technology, Faculty of Chemistry, University of the Basque Country UPV/EHU, Paseo Manuel de Lardizabal 3, Donostia-San Sebastian, 20018, Gipuzkoa, Spain

ARTICLE INFO

Keywords:
Polymer nanocomposites
Melt processing
Carbon nanotubes
Graphene nanoplatelets
Thermoplastic polyurethane
Synergies

ABSTRACT

Hybrid nanocomposites (NCs) based on a bio-based thermoplastic polyurethane (TPU) with multi-walled carbon nanotubes (CNTs) and graphene nanoplatelets (GNPs) as nanofillers, were obtained using a simple melt-mixing method. The effects of a) the GNP:CNT ratio, b) the total nanofiller content, and c) the aspect ratio of the CNTs on both the nanostructure and the thermal, electrical, mechanical, and adhesive properties of the NCs were studied in depth. Synergies were observed in the mechanical and electrical properties of the hybrid NCs when compared to the corresponding binary TPU/GNP and TPU/CNT NCs, regardless of either the GNP:CNT ratio or the aspect ratio of the CNTs. This was attributed to the enhanced dispersion of the GNPs in the presence of CNTs, caused by the intercalation of the two-dimensional graphene nanoplatelets among the one-dimensional carbon nanotubes. Consequently, the resulting conductive network was more efficient, and the reinforcing efficiency of the single nanofillers was improved. The findings of our study show that electrically conductive NCs with improved mechanical properties were achieved when part of the CNTs in the formulation was replaced by cheaper GNPs. Furthermore, a synergy was also observed in the adhesive properties of the hybrid NCs through their significantly higher lap shear strength than that of the pure TPU or binary reference NCs. In other words, by replacing part of the CNTs with GNPs, we were able to obtain hybrid TPU NCs which were cheaper, more effective, and higher performing than binary TPU/CNT and TPU/GNP NCs, pointing to their potential use as electrically conductive hot-melt adhesives.

1. Introduction

Polymer nanocomposites (NCs) with carbon-based nanofillers – both carbon nanotubes (CNTs) and graphene-based fillers (exfoliated graphene, GR; graphene nanoplatelets, GNPs) – have been extensively studied over the last few decades, because, apart from the usual improvements to mechanical, thermal, and other properties, these carbon-based nanofillers make it possible to obtain electrically semi-conductive polymeric materials [1,2]. This semi-conductive state is attained when the so-called percolation threshold is reached, i.e., the minimum concentration of nanofiller necessary for a tridimensional conductive path to be created through the polymer matrix. Several factors are known to determine the final properties of such NCs, such as the geometry of the carbon-based nanofillers (one-dimensional carbon nanotubes vs. two-dimensional graphene), the degree of dispersion, the aspect ratio, and their functionalization to enhance interactions with the polymer matrix.

In a more recent development, the practice of combining different nanofillers (CNTs, GR and GNPs) to produce hybrid NCs has proven an effective way to achieve synergistic mechanical [3–14] and/or electrical properties [3,6,13–19]. While the improved dispersion in hybrid NCs (compared to binary ones) is believed to be at the root of these synergies, different mechanisms have been suggested as actually causing it [5,13]. For example, the long, flexible CNTs in NCs with multilayered graphene are thought to build bridges between the graphene sheets, thus stopping them from restacking. In NCs with exfoliated graphene, on the other hand, the single graphene sheets may be responsible for stopping the CNTs from re-aggregating.

Among the different thermoplastic matrixes used for obtaining hybrid nanocomposites, thermoplastic polyurethanes (TPUs) are deemed promising candidates. This is because their chemical structure, which combines hard and soft segments, allows their properties to be tailored by modifying both their composition and the monomers (isocyanates, alcohols, and chain extenders) used to synthetize them.

* Corresponding author.
E-mail address: gonzalo.gerrika@ehu.eus (G. Guerrica-Echevarria).

https://doi.org/10.1016/j.polymertesting.2023.108068
Received 31 March 2023; Received in revised form 8 May 2023; Accepted 14 May 2023
Available online 15 May 2023

Consequently, TPUs can be used in a wide range of applications, including automotive, electronic, and medical applications. By developing electrically conductive TPU NCs with improved properties, the field of application could be broadened even further. Binary TPU nanocomposites with CNTs [20–22] and with graphene-based nanofillers [23–26] have already been studied. Hybrid TPU nanocomposites have also received attention but to a lesser extent [12,13,27,28].

Li et al. [12] used solvent blending to obtain hybrid TPU NCs containing functionalized graphene-oxide (f-GO) and f-CNTs. The authors observed that, compared to binary NCs, both the nanofillers in the hybrid NCs were homogeneously distributed, and that this created an interconnected 3D path, which, in turn, had a synergistic effect on the mechanical properties of the hybrid NCs.

Rostami et al. [13] also used solution mixing to obtain hybrid TPU NCs with functionalized graphene nanoplatelets (f-GNPs) and nanotubes (f-CNTs). With the total nanofiller content in the NCs set at 3 wt%, the authors analyzed the effect of the f-GNP:f-CNT ratio. The presence of exfoliated GNPs was reported as being responsible for the improved dispersion levels observed in the hybrid NCs, as it prevented re-agglomeration of the nanotubes. Consequently, when the electrical properties of the reference binary NCs and the hybrid NCs containing 3 wt% total nanofiller content were compared, all the hybrid NCs (regardless of the f-GNP:f-CNT ratio) showed negative deviations in the resistivity from what was predicted by the law of mixtures. A synergistic effect was also reported in the mechanical properties, as the modulus, strength, and ductility values of the hybrid NCs were all above the linearity.

Liu et al. [27] employed a co-coagulation method to prepare hybrid TPU nanocomposites with a fixed f-CNT content and varying GR contents. Regarding the electrical properties of the reference binary NCs, the authors reported that the p_c of the binary TPU/GR NCs was lower than that of the TPU/f-CNT NCs due to the quality of the dispersion of GR and its presence in monolayers. In the hybrid NCs, the presence of monolayers of GR helped to disperse the CNTs better. As a result, the p_c of the hybrid NCs was lower than that of the binary TPU/GR NCs.

Finally, Roy et al. [28] obtained hybrid TPU NCs with CNT/GR contents ranging from 0.25 to 1 wt% (with a 1:1 CNT:GR ratio) by solvent mixing. The hybrid NC with 0.5 wt% CNT/GR was finely dispersed, while aggregates of the nanofillers were observed in the hybrid NC containing 1 wt%.

In short, even though hybrid TPU NCs with CNTs and graphene-based nanofillers have been researched, a thorough study analyzing how the total nanofiller content, the composition ratio, and the aspect ratio of the CNTs affect the final mechanical, electrical, and adhesive properties has yet to be conducted. Additionally, solvents were used in all the papers published to date, while melt compounding – which is considered a solvent-free, cost-effective method for mass-producing polymer nanocomposites in industry [14] – was not used in any of the studies. For this reason, melt processing was used in this study to prepare hybrid NCs based on a TPU that is partially derived from renewable resources with CNTs and GNPs as hybrid nanofillers. The total concentration of the nanofillers was varied, as was the GNP:CNT ratio. The effect of the aspect ratio of the CNTs was also studied. The nanostructure and the thermal, mechanical, electrical, and adhesive properties were determined and compared. The corresponding binary NCs were also prepared and characterized as a reference.

2. Experimental

2.1. Materials

A linear, aromatic bio-based polyurethane based on polyol from renewable resources (Pearlbond ® Eco D590, kindly supplied by Merquinsa) was used as the polymer matrix. Two different types of multi-walled carbon nanotubes (CNTs) were employed: Cheap Tubes from Grafton, USA, and NC7000™ from Nanocyl, Belgium (main properties shown in Table 1). Low density graphene nanoplatelets (GNPs, purity 98.5%) under 10 nm thick were acquired from Avanzare (Spain).

2.2. Preparation of the NCs

Hybrid TPU NCs with GNP/CNT contents ranging from 0 to 4 wt% (named TPU-x hereafter, where x represents the total nanofiller content wt%) and ratios of 1:1 and 2:1 GNP:CNT were first mixed by simultaneous extrusion and then injection- or compression-molded to obtain standard test specimens. Binary NCs with the two nanofillers (i.e., TPU/GNP and TPU/CNT) were also obtained as a reference. The compositions studied are shown in Tables 2 and 3. Depending on the system, some additional compositions were prepared in order to build the electrical conductivity curve and calculate the percolation threshold accurately, as necessary.

The extrusions were carried out in a Collin ZK25 co-rotating twin screw extruder-kneader at a melt temperature of 130 °C and a screw rotation speed of 400 rpm. The screw diameter and the L/D ratio were 25 mm and 30, respectively. The extrudates were cooled in a water bath and pelletized. Injection molding was performed in a Battenfeld BA-230 E reciprocating screw injection molding machine to obtain tensile specimens (ASTM D638, type IV, thickness: 1.84 mm). The screw of the plasticization unit was a standard screw with a diameter of 18 mm, L/D ratio of 17.8, and a compression ratio of 4. The melt temperature used was 130 °C, while the mold temperature was 15 °C. The injection speed was 10.2 $cm^3\ s^{-1}$. To carry out the electrical conductivity measurements, circular sheets measuring 70 mm Ø and 1.1 mm thick were obtained by compression molding at 130 °C using a Collin P200E press. The specimens were left to condition for 24 h in a desiccator before analyzing and testing.

2.3. Characterization and testing

The melting and crystallization behavior of the binary and hybrid TPU NCs was studied by DSC in a PerkinElmer DSC-7 calorimeter calibrated with an Indium standard. The temperature range analyzed was 0 °C to 100 °C, and each sample was subjected to a heating-cooling-heating cycle at a rate of 20 °C/min. The melting temperature (T_m) and enthalpy (ΔH_m) of the TPU were determined from the second heating scans using the peak maximum and area, respectively. The crystallization temperature (T_c) was determined from the cooling scans. Dynamic mechanical analysis was carried out in a TA Instruments DMA Q800 apparatus that provided the tanδ vs. temperature plots. The scans were performed from −100 °C to 60 °C at a constant heating rate of 4 °C/min and at a frequency of 1 Hz.

The degree of nanofiller dispersion was analyzed by TEM. To obtain the samples, the central part of the tensile specimens was ultrathin-sectioned at 30–40 nm using a cryo-ultramicrotome. The micrographs were obtained in a Tecnai G2 20 Twin microscope at an accelerating voltage of 200 kV.

The electrical conductivity was determined by means of a digital picoammeter (Keithley), where a voltage of 0.1 V was applied to the samples for 1 min and the passing intensity was measured and converted into volumetric electrical conductivity (σ) using Eq. (1).

$$\sigma = \frac{1}{\rho} = \frac{t \cdot I}{22.9 \cdot V} \tag{1}$$

where ρ is the resistivity, t is the thickness of the sample, I is the intensity of the current, V is the voltage applied, and 22.9 is the specific area of the electrodes. The percolation threshold was determined by means of Eq. (2).

$$\sigma(p) = B(p - p_c)^t \tag{2}$$

where $\sigma(p)$ is the experimental conductivity, B is a proportionality constant, t is the critical exponent, p is the nanofiller concentration, and

Table 1
Properties of the CNT used.

Sample	Abbreviation	Nominal diameter (nm)	Nominal length (μm)	Specific surface area (m^2/g)	Carbon purity (%)	Post-processing aspect ratio (L/D)[a]
Cheaptubes	CNT^1	20–30	10–30	110	>95	18
Nanocyl	CNT^2	9.5	1.5	250–300	90	25

[a] See Otaegi et al. [29].

Table 2
The hybrid NCs in the study and their composition.

COMPOSITION	NANOFILLER wt%	GNPs wt%	CNTs wt%
TPU-1 GNP/CNT^1 (1:1)	1	0.5	0.5
TPU-2 GNP/CNT^1 (1:1)	2	1	1
TPU-3 GNP/CNT^1 (1:1)	3	1.5	1.5
TPU-4 GNP/CNT^1 (1:1)	4	2	2
TPU-1 GNP/CNT^1 (2:1)	1	0.667	0.333
TPU-2 GNP/CNT^1 (2:1)	2	1.333	0.667
TPU-3 GNP/CNT^1 (2:1)	3	2	1
TPU-4 GNP/CNT^1 (2:1)	4	2.667	1.333
TPU-1 GNP/CNT^2 (1:1)	1	0.5	0.5
TPU-2 GNP/CNT^2 (1:1)	2	1	1
TPU-3 GNP/CNT^2 (1:1)	3	1.5	1.5
TPU-4 GNP/CNT^2 (1:1)	4	2	2
TPU-1 GNP/CNT^2 (2:1)	1	0.667	0.333
TPU-2 GNP/CNT^2 (2:1)	2	1.333	0.667
TPU-3 GNP/CNT^2 (2:1)	3	2	1
TPU-4 GNP/CNT^2 (2:1)	4	2.667	1.333

Table 3
The reference binary NCs and their composition.

COMPOSITION	NANOFILLER wt%
TPU	–
TPU-1 GNP	1
TPU-2 GNP	2
TPU-3 GNP	3
TPU-4 GNP	4
TPU-1 CNT^1	1
TPU-2 CNT^1	2
TPU-3 CNT^1	3
TPU-4 CNT^1	4
TPU-1 CNT^2	1
TPU-2 CNT^2	2
TPU-3 CNT^2	3
TPU-4 CNT^2	4

p_c is the percolation threshold. The experimental results were fitted by plotting $\log(\sigma)$ vs. $\log(p\text{-}p_c)$ and incrementally varying p_c until the best linear fit was obtained.

Tensile testing was carried out using an Instron 5569 machine at a cross-head speed of 50 mm/min, a temperature of 23±2 °C, and 50 ± 5% relative humidity. A minimum of five tensile specimens were tested for each reported value.

The adhesive bond strength of the hybrid TPU NCs was determined by single lap shear tests performed in an Instron 5569 machine at a cross-head speed of 1 mm/min. Thin aluminum (Al) plates were used as substrates for preparing joints bonded by the hybrid NCs. The Al plates had nominal dimensions of 140 × 25 × 0.8 mm^3, and the joint area was approximately 25 × 25 mm^2 and 0.1 mm thick (Fig. 1). Prior to the bonding, the Al plates were cleaned with acetone. The joint samples were obtained by hot-pressing at 130 °C using a Collin P200E press. Ten samples were tested for each reported value. Lap shear tests of the neat TPU and the binary TPU/GNP and TPU/CNT NCs were also performed as a reference.

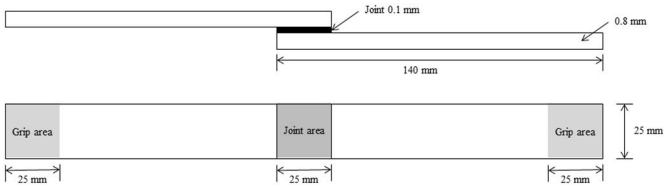

Fig. 1. Schematic representation of the single lap shear test samples.

3. Results and discussion

3.1. Thermal properties

The amorphous phase characteristics of the TPU in the hybrid NCs were analyzed by DMTA. As an example, the tanδ vs. T curves of the hybrid TPU GNP/CNT^1 (2:1) NCs and the neat TPU are shown in Fig. 2. All the hybrid NCs studied showed similar characteristics; the corresponding curves are shown in Fig. S1. The values of the T_gs of the hybrid NCs, determined from the maximum of the tanδ vs. T curves, are summarized in Table 4. For comparison purposes, Table 5 shows the corresponding values for the binary NCs. As Table 5 shows, there was a slight increase in the T_g when GNPs were added to the TPU (from −20.5 °C in the pure TPU to a maximum of −18 °C for the NC containing 4 wt% GNP content). More significant increases in the T_g were observed in the binary NCs that contained CNTs (the maximum T_g values for CNT^1 and CNT^2 were −11.5 °C and −12.5 °C, respectively). These results point to the CNTs being more effective than the GNPs in restraining the molecular mobility of the TPU chains, which, according to the literature, is the most widely reported effect of carbon-based nanofillers on the T_g [26,29–32]. Therefore, the difference between the two nanofillers must be related either to their different geometry or to the degree of dispersion in each case, as will be discussed in the next section.

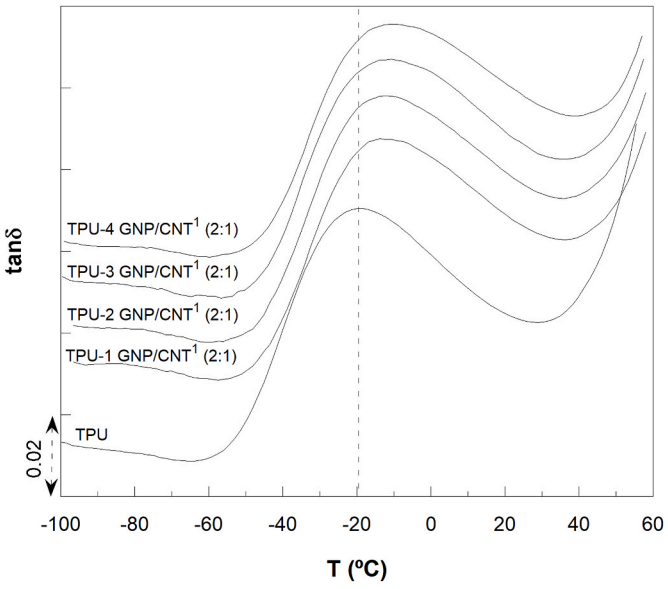

Fig. 2. Tanδ vs. temperature curves of the hybrid TPU GNP/CNT^1 (2:1) nanocomposites. The curves have been shifted along the y axis for clarity.

Table 4
Melting, crystallization and glass transition temperatures, and melting enthalpy of the hybrid NCs.

COMPOSITION	T_m (°C)[a]	ΔH_m (J/g)[a]	T_c (°C)[a]	T_g (°C)[b]
TPU	67.5	75	37.0	−20.5
TPU-1 GNP/CNT^1 (1:1)	68.0	80	43.0	−17.5
TPU-2 GNP/CNT^1 (1:1)	67.0	70	43.5	−17.0
TPU-3 GNP/CNT^1 (1:1)	67.0	70	46.0	−16.5
TPU-4 GNP/CNT^1 (1:1)	67.0	65	46.5	−16.0
TPU-1 GNP/CNT^1 (2:1)	68.0	75	44.0	−14.5
TPU-2 GNP/CNT^1 (2:1)	68.5	70	45.5	−14.0
TPU-3 GNP/CNT^1 (2:1)	68.5	70	46.5	−12.0
TPU-4 GNP/CNT^1 (2:1)	68.5	70	47.0	−11.5
TPU-1 GNP/CNT^2 (1:1)	72.0	75	46.0	−15.0
TPU-2 GNP/CNT^2 (1:1)	72.0	75	47.5	−14.5
TPU-3 GNP/CNT^2 (1:1)	72.0	75	47.0	−14.0
TPU-4 GNP/CNT^2 (1:1)	70.0	75	47.0	−10.0
TPU-1 GNP/CNT^2 (2:1)	71.0	75	44.0	−14.5
TPU-2 GNP/CNT^2 (2:1)	71.0	80	46.5	−14.0
TPU-3 GNP/CNT^2 (2:1)	72.0	70	46.5	−12.5
TPU-4 GNP/CNT^2 (2:1)	71.0	75	46.0	−13.0

The standard deviation was ±0.5 °C for the melting and crystallization temperatures and 5% for the melting enthalpy.
[a] Obtained by DSC.
[b] Obtained by DMTA.

Table 5
Melting, crystallization and glass transition temperatures, and melting enthalpy of the neat TPU and the binary NCs with CNTs and GNPs.

COMPOSITION	T_m (°C)[a]	ΔH_m (J/g)[a]	T_c (°C)[a]	T_g (°C)[b]
TPU	67.5	75	37.0	−20.5
TPU-1 GNP	67.5	65	44.0	−19.0
TPU-2 GNP	67.5	65	44.0	−18.5
TPU-3 GNP	67.5	65	44.5	−18.0
TPU-4 GNP	68.5	60	45.5	−18.0
TPU-1 CNT^1	68.0	75	43.5	−14.0
TPU-2 CNT^1	67.0	75	43.5	−12.5
TPU-3 CNT^1	69.0	80	46.0	−12.5
TPU-4 CNT^1	69.0	80	46.0	−11.5
TPU-1 CNT^2	72.0	75	44.0	−14.0
TPU-2 CNT^2	73.0	75	44.5	−13.0
TPU-3 CNT^2	72.5	75	46.5	−13.5
TPU-4 CNT^2	72.0	75	47.0	−12.5

The standard deviation was ±0.5 °C for the melting and crystallization temperatures and 5% for the melting enthalpy.
[a] Obtained by DSC.
[b] Obtained by DMTA.

Regarding the hybrid NCs, similar results to those of the binary NCs were observed, with maximum T_g values ranging from −16.0 °C to −10.0 °C, depending on the GNP/CNT ratio and type of CNTs used. This is probably due to the combined effect of the GNPs and CNTs on the molecular mobility of the TPU. Interestingly, in the hybrid NCs having a GNP:CNT ratio of 2:1 the displayed T_gs were higher than those of the binary TPU/GNP NCs and approximately as high as those of the corresponding binary TPU/CNT NCs. This could be indicative of a better dispersion degree of the GNPs in the hybrid NCs, which will be further discussed in the next sections, leading to a greater restriction on the molecular mobility of the TPU.

The crystalline characteristics of the TPU in the hybrid and binary NCs were analyzed by DSC and the results are shown in Tables 4 and 5, respectively. As can be seen, the melting temperature (T_m) and enthalpy (ΔH_m), corresponding to the crystallization of the hard segment of the TPU and determined from the second heating scan, hardly changed in either the hybrid or binary NCs when the nanofiller was added. Only slight increases in the T_m were observed when CNT^2 was present in both the hybrid and binary NCs. This has been attributed to the nucleating effect of nanofillers and the formation of more perfect crystals [30]. Nevertheless, the most common result in the literature is that no change occurs in the melting behavior of polymers when carbon-based nanofillers are added [33].

Fig. 3 shows the cooling thermograms of the hybrid TPU GNP/CNT^1 (2:1) NCs as an example. The other hybrid NCs in the study showed similar curves and are shown in Fig. S2. Table 4 summarizes the T_c of the TPU in the hybrid NCs, whereas Table 5 shows the T_c of the reference binary NCs. As can be observed, the T_c of the hybrid NCs increased at increasing nanofiller contents, as was expected given the nucleating effect observed in the binary NCs in this study (Table 5) as well as in the literature [31,32]. However, as stated before, this nucleating effect did not affect the melting enthalpy of the TPU in the hybrid NCs, indicating that the overall degree of crystallization remained unchanged.

3.2. Nanostructure

The dispersion of the nanofillers in the TPU matrix was analyzed by TEM. The micrographs of the binary NCs with 1 wt% CNT^1, CNT^2 and GNP contents are shown in Fig. 4 a), b), and c), respectively, and those of the hybrid NCs with 1 wt% 1:1 GNP/CNT^1, 2:1 GNP/CNT^1, 1:1 GNP/CNT^2, and 2:1 GNP/CNT^2 are set out in Fig. 5 a, b, c, and d, respectively.

Regarding the binary NCs, the effect of the type of filler (GNPs vs. CNTs) and the aspect ratio of the CNTs (CNT^1 vs. CNT^2) both need to be discussed. Regarding the former, when Fig. 4 c) is compared with Fig. 4 a) and b), it can be seen through the large agglomerates and scarce individual graphene nanolayers of the GNPs, that they are not as well dispersed as the CNTs, which are mainly individually dispersed in both the CNT^1 and CNT^2-based NCs. The superior dispersion of CNTs has also been reported in the literature in studies where the nanostructure of NCs with different carbon-based nanofillers were compared [33]. With respect to the different types of CNTs used in this study, and although – as we mentioned before – the degree of dispersion is good in both cases, Fig. 4 b) shows a percolated or close-to-percolated nanostructure, while Fig. 4 a) shows that the percolation of the CNT^1 nanofiller still has a long way to go. Two factors may account for this difference in behavior: the more effective post-processing aspect ratio and lower density of CNT^2 compared to CNT^1 [34,35], which means more nanotubes per volume unit. Similar results were obtained in a previous study involving NCs

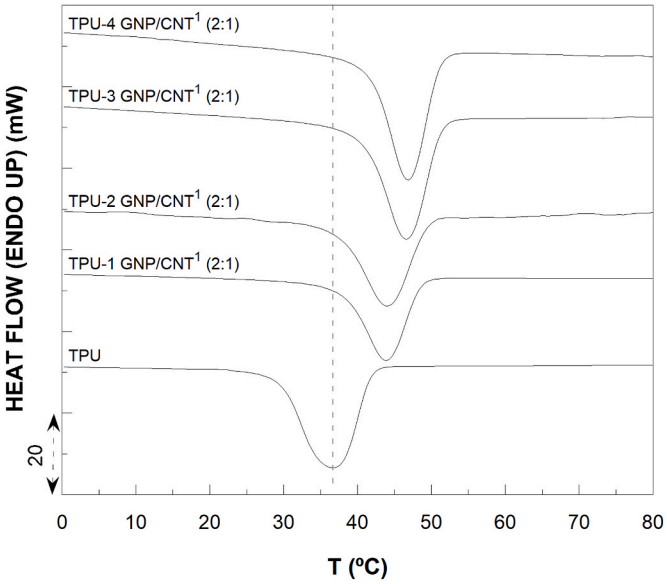

Fig. 3. DSC cooling endotherms of the hybrid TPU GNP/CNT^1 (2:1) nanocomposites. The curves have been shifted along the y axis for the purpose of clarity.

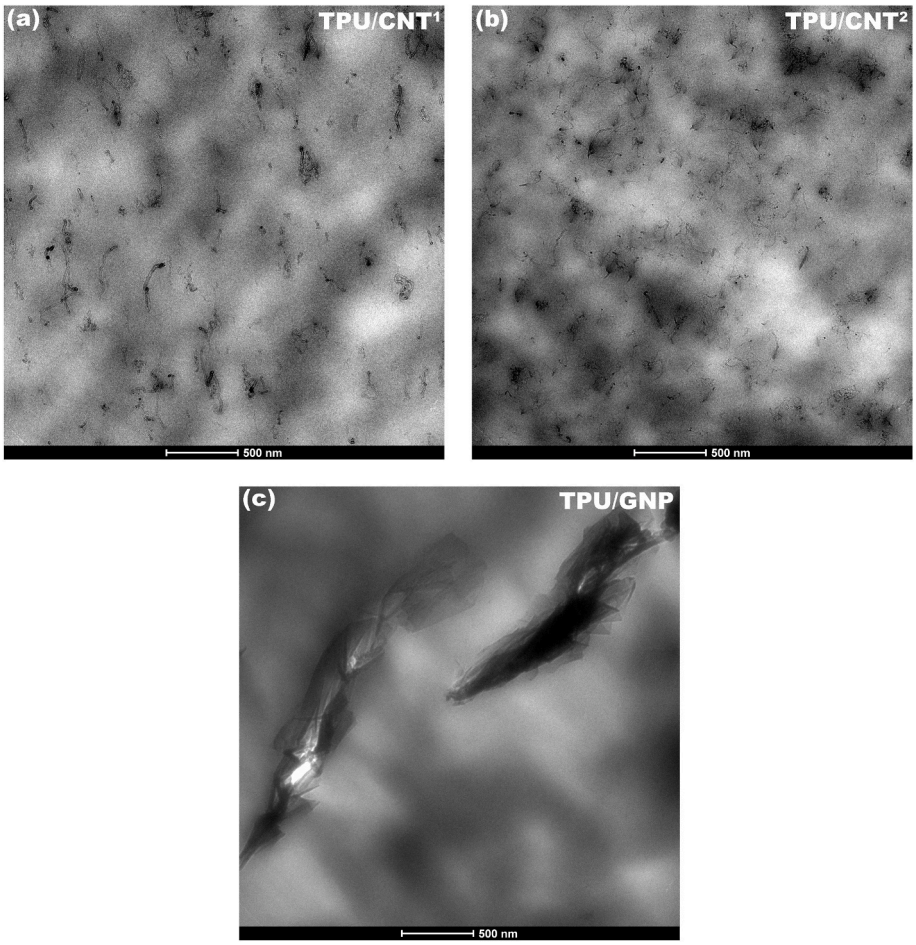

Fig. 4. TEM micrographs of binary a) TPU/CNT[1], b) TPU/CNT[2], and c) TPU/GNP NCs containing 1 wt% nanofiller content at x14500 magnification.

based on a bio-based polyamide and the same types of CNTs as in our study [29].

The results in Fig. 5 are particularly noteworthy. When the micrographs of the hybrid NCs in Fig. 5 a) and b) are compared with those of the binary NCs in Fig. 4 a) on the one hand, and, Fig. 5 c) and d) are compared with Fig. 4 b) on the other – and when the smaller number of CNTs in the hybrid NCs are taken into account, no significant differences were observed in the dispersion levels of either the CNTs[1] or the CNTs[2] when the GNPs were present in the system. Regarding the dispersion of the GNPs, when Fig. 5 a), b), c), and d), are compared with Fig. 4 c), the improvement in the hybrid NCs is clear to see, and is attributed to the presence of the CNTs, which helped to disperse the GNP particles which appear in mostly single nanolayers, unlike the stacked agglomerates of the binary TPU/GNP NCs.

In the literature, the dispersion of the nanofillers in hybrid NCs that contain both CNTs and graphene-based nanofillers has been reported to be better than in NCs with single nanofillers, [3–5,12,27,36]. Two possible mechanisms have been suggested to explain this behavior [5,13]: in NCs with multilayered graphene, the long and flexible CNTs may be able to bridge the distances between the graphene sheets, effectively acting as chelating arms between them and preventing their restacking; while in NCs with exfoliated graphene, the single graphene sheets may prevent the CNTs from re-aggregating. Either way, the addition of hybrid nanofillers can result in the 2-D graphene nanoplatelets intercalating among the 1-D carbon nanotubes, creating a more effective conductive network [27] which, in turn, leads to better electrical and mechanical properties than in NCs with single nanofillers, as shown and discussed below.

3.3. Electrical properties

The electrical conductivity of the binary and hybrid NCs as a function of the nanofiller content is shown in Fig. 6. For the sake of clarity, only the values of the hybrid NCs with a GNP:CNT ratio of 2:1 are shown; the NCs with the 1:1 ratio showed similar values. The electrical percolation thresholds (p_cs) of the studied NCs – i.e., the minimum concentration at which a nanofiller network is created – were fitted using the power law function [37], and the results are shown in Fig. 7 a) for the CNT[1]-based system, and in 7 b) for the CNT[2]-based system.

As can be seen in Fig. 6 and as expected, TPU is an insulating polymer, with an electrical conductivity of $2{\cdot}10^{-14}$ S/cm. The addition of carbon-based nanofillers led to a sharp increase in the electrical conductivity in all cases due to the formation of a conductive path. This occurred at nanofiller contents ranging from 0.4 to 3.9 wt%, depending on the system, and led to conductivity values 7 orders of magnitude higher.

As can be seen in Figs. 6 and 7, when the binary NCs with CNTs were compared with the binary NCs with GNPs, the electrical properties of the former were better and showed a significantly lower p_c and higher electrical conductivity values. This behavior has also been observed in other systems where the effect of GNPs and CNTs on the electrical properties was compared [13,15–17,38–41]. The differences in dispersion and geometry would seem to explain the enhanced electrical properties of the binary TPU/CNT NCs, as the CNTs were significantly better dispersed and were one-dimensional [15,38,39]. Moreover, the fact that there was more contact resistance among the GNPs than among the CNTs could also be a contributing factor [39].

When the binary NCs with the different aspect ratio CNTs were

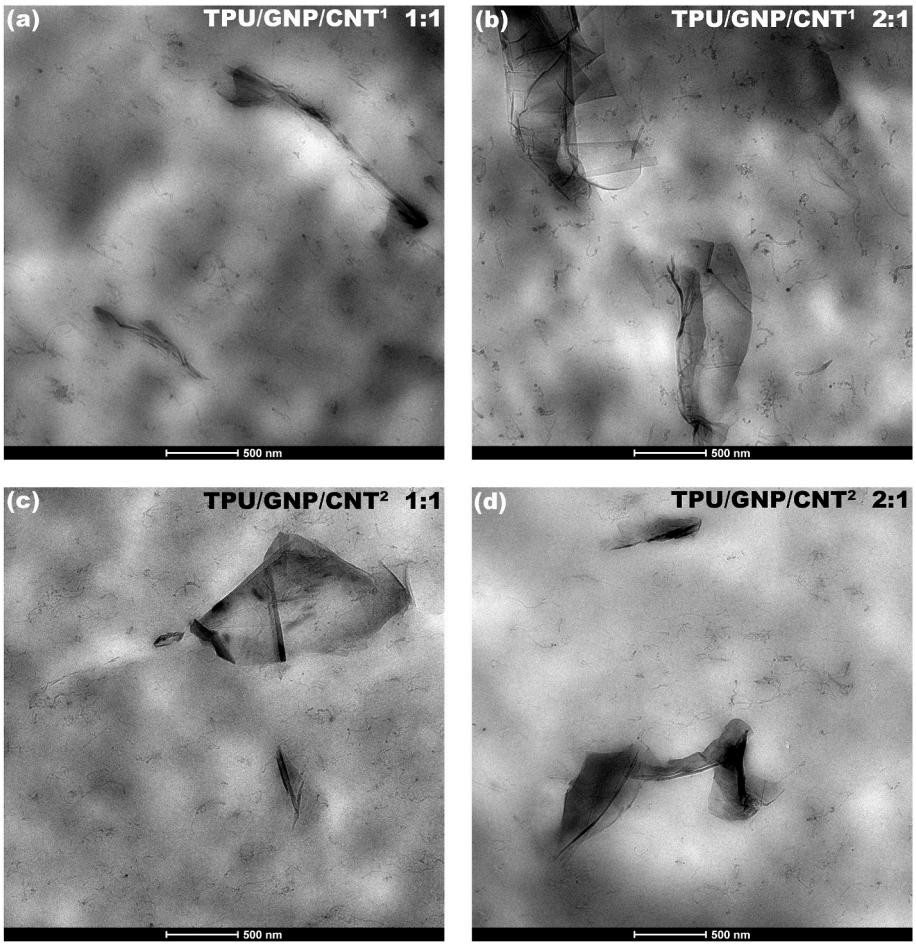

Fig. 5. TEM micrographs of hybrid TPU NCs containing 1 wt% nanofiller content at x14500 magnification. a) GNP/CNT^1 1:1, b) GNP/CNT^1 2:1, c) GNP/CNT^2 1:1, and d) GNP/CNT^2 2:1.

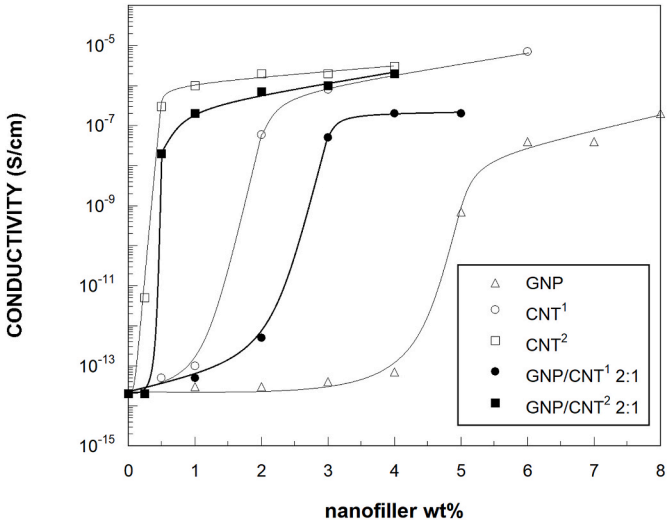

Fig. 6. Electrical conductivity of the studied binary and hybrid TPU NCs, as a function of the nanofiller content.

compared, Figs. 6 and 7 show that the p_c of the NC containing CNTs^2 is significantly lower than that of the NC containing CNTs^1 (0.44 vs. 1.66 wt% content). This behavior is consistent with the nanostructure observed by TEM and discussed in the previous section (Fig. 4 a) and b)). Similar results were obtained elsewhere for bio-polyamide-based nanocomposites [29].

Fig. 7 shows that the p_cs of the hybrid NCs were almost as low as those of the binary TPU/CNT NCs regardless of the GNP:CNT ratio and, therefore show a clear negative deviation from the linear behavior (shown by the dotted line in Fig. 7 a) and b)). Moreover, a similar synergy can also be observed in Fig. 8, which shows the electrical conductivity values of the hybrid and binary NCs with 4 wt% nanofiller content. The effects were even more significant in the hybrid NCs containing CNT^2, indicating that the higher the effective aspect ratio and the nanotubes-per-volume unit of the CNTs, the greater the synergistic effect in hybrid NCs.

The conductivity values obtained in this work are close to the ones reported for TPU GNP-CNT hybrid NCs obtained by solution blending: around 10^{-6} S/cm for the hybrid TPU NCs having 0.255 vol% f-CNT and 0.006 vol% GR [27], and 10^{-4} S/cm for TPU f-GNP:f-CNT hybrid NCs with a total content of nanofillers of 3 wt% [13]. Besides, Rostami et al. [13] calculated the predicted p_c of the TPU f-GNP:f-CNT hybrid NC considering the values shown by the corresponding binary ones (1.18 wt % and 0.39 wt% for f-GNP and f-CNT, respectively). They reported calculated p_cs of 0.78 wt%, 0.59 wt% and 0.47 wt% for hybrid NCs with f-GNP:f-CNT ratios of 3:1, 2:2, and 1:3, respectively. Therefore, even though the reported p_c-s for the binary NCs are lower to those obtained in this work, probably owing to the functionalization of the nanofillers, the p_c of the hybrid NCs obtained with CNT^2 is lower, indicating that the synergism attained in this work was greater.

Synergies between the p_c and the electrical conductivity of hybrid GNP-CNT NCs have also been observed in other systems [3,6,13,15–19]. There are two main reasons for this behavior: i) a more efficient

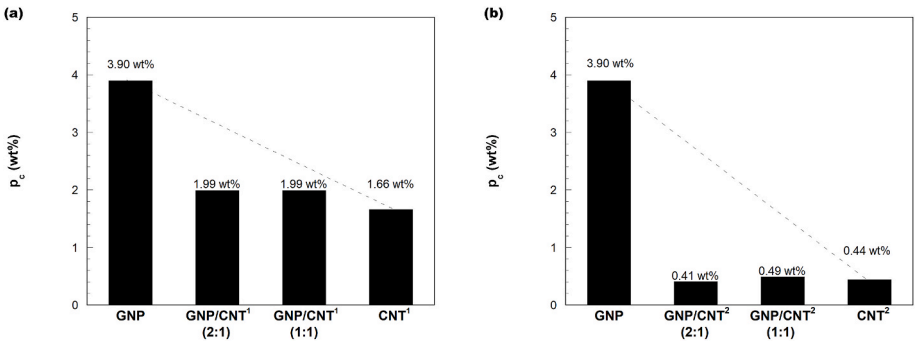

Fig. 7. Electrical percolation threshold of the studied binary and hybrid TPU NCs. a) the CNT^1-based systems and b) the CNT^2-based systems.

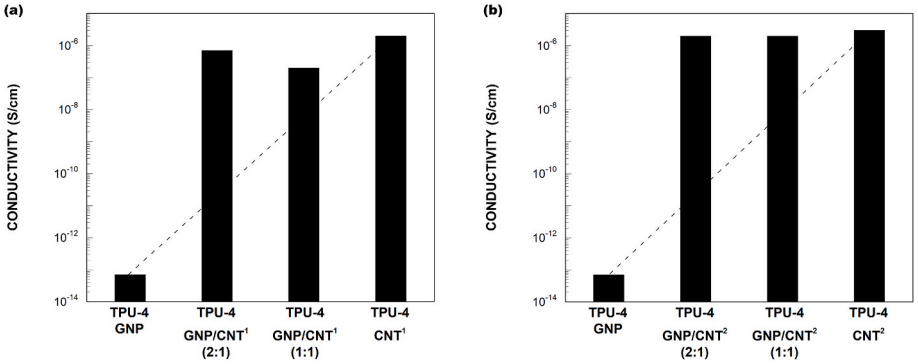

Fig. 8. Electrical conductivity of the hybrid and binary TPU NCs with 4 wt% nanofiller content. a) CNT^1-based systems and b) CNT^2-based systems.

percolated network is formed when nanofillers with different geometries are combined, which facilitates the transport of electrons in the hybrid conductive pathways where the CNTs act as bridges among the GNPs, effectively reducing the gap between the conductive nanofillers [3,38,42]; and ii) the presence of CNTs improves the dispersion of the GNPs [38,42]. The higher aspect ratio and lower density of the $CNTs^2$ also played an important role in the synergies observed.

This is noteworthy because these synergies make it possible to produce electrically conductive TPU NCs with very low nanofiller contents, and more importantly, it means that GNPs can be used instead of a portion of the more expensive CNTs.

3.4. Mechanical properties

The mechanical properties of the hybrid and binary TPU NCs were measured by tensile tests, the results of which are summarized in Tables 6 and 7, respectively. Fig. 9 shows Young's modulus for the binary and hybrid NCs with a 4 wt% nanofiller content.

As was expected and is shown in Tables 6 and 7, increasing concentrations of both binary and hybrid nanofillers led to increasing Young's moduli and yield strength values, and decreasing ductility values [12,24,43].

Regarding the reinforcing efficiency of CNTs and GNPs in the binary TPU NCs, based on the observed nanostructure, the enhanced dispersion of the CNTs in the NCs led to higher Young's modulus and yield strength values when NCs with the same amount of CNTs and GNPs were compared. The greater surface area of the different geometries may also have helped to achieve a more effective load transfer from the polymer to the nanofiller. Also as expected, the NCs with the $CNTs^2$ showed slightly higher Young's modulus and yield strength values. Considering the usual stress concentrating effect of nanofillers and the consequent negative effect on ductility, it should be highlighted that all the NCs in this study showed a ductile behavior, with high elongation at break values.

If the Young's moduli of the hybrid and binary NCs are compared (Fig. 9), the synergistic behavior of the hybrid NCs is clearly reflected through the Young's modulus values which are higher than those predicted by the additivity rule (see the dotted line). As in the electrical properties discussed above, this effect is more noticeable in the hybrid NCs containing the $CNTs^2$. The GNP/CNT ratio did not seem to have a significant effect on the final properties of the hybrid NCs.

Similar results have been reported on TPU hybrid NCs obtained by solution blending. Li et al. [12] attained maximum improvements of 134% and 92% in the Young's modulus and the tensile strength of neat TPU when 1 wt% of f-GO:f-CNT was added, whereas higher hybrid nanofiller contents led to lower mechanical properties. The improvements observed by Rostami et al. [13] were of 86% and 30%, respectively, in the case of the TPU hybrid NCs containing a total nanofiller concentration of 3%, with a f-GNP:f-CNT ratio of 3:1.

Synergistic behaviors following the addition of hybrid nanofillers have already been reported in systems with other polymers [3–11], including TPUs [12,13], as matrices. As with the electrical properties, the synergistic effect here is attributed to the improvement observed in the nanostructure, where the presence of nanotubes prevented re-agglomeration of the graphene layers, increasing the aspect ratio and the available contact area between the nanofillers and the polymer matrix as a result. The reason for the greater synergy of the hybrid NCs with $CNTs^2$ is attributed to their higher aspect ratio on the one hand, and their higher volume content, on the other.

In conclusion, an outstanding reinforcing effect was achieved by adding hybrid nanofillers to TPU. The hybrid NCs showed significantly higher Young's moduli – up to 82% higher – than those of the neat TPU or even the binary NCs, while maintaining the ductile nature of the matrix.

3.5. Adhesive properties

The results of the lap shear tests used to measure the adhesive

Table 6
Young's modulus, yield strength, and ductility, measured as the elongation at break of the hybrid NCs.

COMPOSITION	YOUNG'S MODULUS (MPa)	YIELD STRENGTH (MPa)	DUCTILITY (%)
TPU-1 GNP/CNT[1] (1:1)	540	14.2	520
TPU-2 GNP/CNT[1] (1:1)	550	13.7	480
TPU-3 GNP/CNT[1] (1:1)	610	14.6	360
TPU-4 GNP/CNT[1] (1:1)	640	15.4	340
TPU-1 GNP/CNT[1] (2:1)	580	15.1	480
TPU-2 GNP/CNT[1] (2:1)	630	15.7	360
TPU-3 GNP/CNT[1] (2:1)	670	16.3	360
TPU-4 GNP/CNT[1] (2:1)	720	16.4	340
TPU-1 GNP/CNT[2] (1:1)	553	15.6	389
TPU-2 GNP/CNT[2] (1:1)	673	17.4	357
TPU-3 GNP/CNT[2] (1:1)	741	18.1	344
TPU-4 GNP/CNT[2] (1:1)	819	18.7	316
TPU-1 GNP/CNT[2] (2:1)	598	15.5	460
TPU-2 GNP/CNT[2] (2:1)	676	16.3	379
TPU-3 GNP/CNT[2] (2:1)	747	16.7	346
TPU-4 GNP/CNT[2] (2:1)	837	17.3	334

The standard deviation was ±10 MPa, 0.5 MPa and 20% for Young's modulus, the yield strength, and the ductility, respectively.

Table 7
Young's modulus, the yield strength, and the ductility, measured as the elongation at break of the neat TPU and the binary NCs with CNTs, and with GNPs.

COMPOSITION	YOUNG'S MODULUS (MPa)	YIELD STRENGTH (MPa)	DUCTILITY (%)
TPU	460	13.6	560
TPU-1 GNP	470	12.3	460
TPU-2 GNP	500	12.8	410
TPU-3 GNP	580	13.4	360
TPU-4 GNP	620	13.2	340
TPU-1 CNT[1]	540	15.0	520
TPU-2 CNT[1]	570	15.6	480
TPU-3 CNT[1]	590	16.0	420
TPU-4 CNT[1]	610	16.3	400
TPU-1 CNT[2]	575	15.5	420
TPU-2 CNT[2]	603	15.6	366
TPU-3 CNT[2]	642	15.9	350
TPU-4 CNT[2]	710	16.8	293

The standard deviation was ±10 MPa, 0.5 MPa and 20% for Young's modulus, the yield strength and the ductility, respectively.

properties of the hybrid and binary TPU NCs with 4 wt% nanofiller content are shown in Fig. 10. The lap shear strength of the neat TPU is also provided as a reference.

The addition of GNPs to the TPU led to a slight decrease in the adhesive properties of the binary NCs. By contrast, the addition of CNTs resulted in higher lap shear strength values. Whenever the effect of carbon-based nanofillers on the adhesive properties has been discussed in the literature to date, the polymer matrices in question were usually epoxy resins [44–47], and the carbon-based nanofillers generally led to an improvement of the adhesive properties. However, decreases have also been observed when GNPs were added.

Regarding the adhesive properties of the hybrid NCs compared with the binary NCs, the former clearly showed values above the additivity law, indicating that, in addition to the synergies in the mechanical and electrical properties, a synergistic effect on the adhesive properties of the hybrid NCs was also observed.

4. Conclusions

In this study, hybrid bio-based thermoplastic polyurethane nanocomposites containing CNTs and GNPs were found to exhibit synergies in mechanical, electrical, and adhesive properties. The following main conclusions can be drawn.

- Given the effect of adding GNPs or CNTs separately, the addition of hybrid nanofillers caused an increase in both the glass transition temperature and the crystallization temperature of the NCs, as expected.
- TEM observations showed that the dispersion of the GNPs in the hybrid NCs improved, and that the resulting nanostructure led to lower percolation thresholds and higher electrical conductivity values than those predicted by the rule of mixtures. In other words, a synergy in the electrical properties was observed.
- The mechanical properties also exhibited synergistic behavior: NCs with a considerably higher Young's modulus and yield strength than the neat TPU were obtained while maintaining their ductile behavior.
- The GNP:CNT ratio did not seem to have any significant effect on the final electrical and mechanical properties of the hybrid NCs, suggesting that cheaper GNPs can be used to replace up to 2/3 of the CNTs in the formulation.
- The type of CNTs used had a substantial effect on the final properties of the binary and hybrid NCs. CNTs with a higher post-processing aspect ratio and lower density dispersed better, resulting in superior electrical and mechanical properties.
- A synergy in the adhesive properties of the hybrid NCs was also observed and measured with lap-shear tests.

So, instead of using binary TPU/CNT and TPU/GNP NCs, more efficient, higher performing, more affordable bio-based NCs can be obtained by replacing part of the more expensive CNTs with the less expensive GNPs, thus laying the groundwork for the use of hybrid TPU NCs as electrically conductive, hot-melt adhesives.

Author statement

Nora Aranburu: Conceptualization, Investigation, Writing - original draft, Writing - review & editing. **Itziar Otaegi**: Conceptualization, Investigation, Writing - original draft, Writing - review & editing. **Gonzalo Guerrica-Echevarria**: Conceptualization, Investigation, Writing - original draft, Writing - review & editing.

Funding

This research was funded by the Basque Government through project IT1503-22.

Declaration of competing interest

The authors declare that they have no known competing financial interests or personal relationships that could have appeared to influence the work reported in this paper.

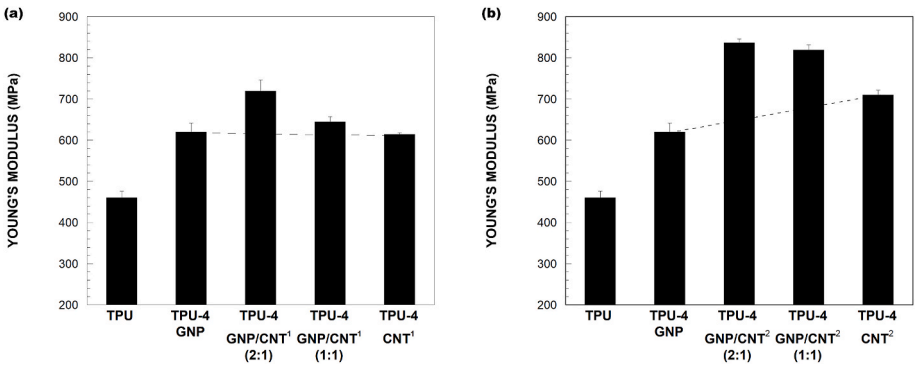

Fig. 9. Young's modulus of the hybrid and binary TPU NCs with 4 wt% nanofiller content. The value of pure TPU has also been included for comparison purposes. a) CNT^1-based systems and b) CNT^2-based systems.

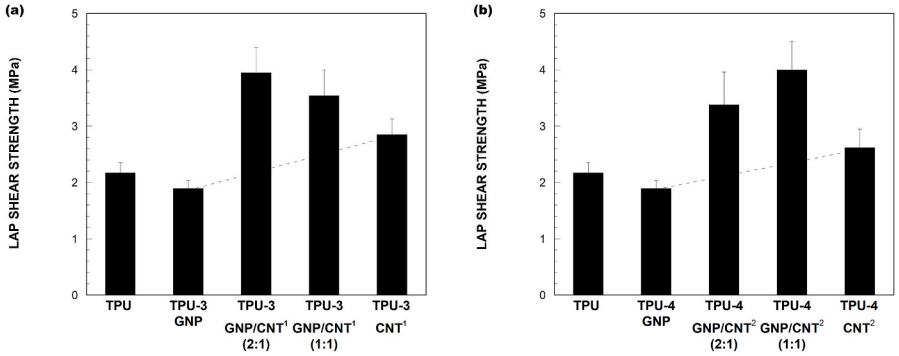

Fig. 10. Lap shear strength of the hybrid and binary TPU NCs with 4 wt% nanofiller content. a) CNT^1-based systems and b) CNT^2-based systems.

Data availability

No data was used for the research described in the article.

Acknowledgements

The authors are grateful for the technical and human support provided by SGIker (UPV/EHU/ERDF, EU).

Appendix A. Supplementary data

Supplementary data to this article can be found online at https://doi.org/10.1016/j.polymertesting.2023.108068.

References

[1] D.N. Trivedi, N.V. Rachchh, Graphene and its application in thermoplastic polymers as nano-filler- A review, Polymer 240 (2022), 124486, https://doi.org/10.1016/j.polymer.2021.124486.
[2] B.P. Grady, in: Carbon Nanotube-Polymer Composites: Manufacture, Properties, and Applications, John Wiley & Sons, Hoboken, 2011, https://doi.org/10.1002/9781118084380.
[3] L. Yue, G. Pircheraghi, S.A. Monemian, I. Manas-Zloczower, Epoxy composites with carbon nanotubes and graphene nanoplatelets - dispersion and synergy effects, Carbon 78 (2014) 268–278, https://doi.org/10.1016/j.carbon.2014.07.003.
[4] S.-Y. Yang, W.-N. Lin, Y.-L. Huang, H.-W. Tien, J.-Y. Wang, C.-C.M. Ma, S.-M. Li, Y.-S. Wang, Synergetic effects of graphene platelets and carbon nanotubes on the mechanical and thermal properties of epoxy composites, Carbon 49 (2011) 793–803, https://doi.org/10.1016/j.carbon.2010.10.014.
[5] A. Rostami, H. Nazockdast, M. Karimi, Graphene induced microstructural changes of PLA/MWCNT biodegradable nanocomposites: rheological, morphological, thermal and electrical properties, RSC Adv. 6 (2016) 49747–49759, https://doi.org/10.1039/c6ra08345e.
[6] M.W. Ahmad, B. Dey, A.A. Sammar, A. Choudhury, In situ synthesis of graphene oxide in multi-walled carbon nanotube hybrid-reinforced polyetherimide nanocomposites with improved electrical, mechanical and thermal properties, Adv. Compos. Mater. 29 (2020) 529–546, https://doi.org/10.1080/09243046.2019.1710680.
[7] S. Chatterjee, F. Nafezarefi, N.H. Tai, L. Schlagenhauf, F.A. Nüesch, B.T.T. Chu, Size and synergy effects of nanofiller hybrids including graphene nanoplatelets and carbon nanotubes in mechanical properties of epoxy composites, Carbon 50 (2012) 5380–5386, https://doi.org/10.1016/j.carbon.2012.07.021.
[8] K.E. Prasad, B. Das, U. Maitra, U. Ramamurty, C.N.R. Rao, Extraordinary synergy in the mechanical properties of polymer matrix composites reinforced with 2 nanocarbons, Proc. Natl. Acad. Sci. U.S.A. 106 (2009) 13186–13189, https://doi.org/10.1073/pnas.0905844106.
[9] S. Paszkiewicz, A. Szymczyk, X.M. Sui, H.D. Wagner, A. Linares, T.A. Ezquerra, Z. Roslaniec, Synergetic effect of single-walled carbon nanotubes (SWCNT) and graphene nanoplatelets (GNP) in electrically conductive PTT-block-PTMO hybrid nanocomposites prepared by in situ polymerization, Compos. Sci. Technol. 118 (2015) 72–77, https://doi.org/10.1016/j.compscitech.2015.08.011.
[10] S. Doagou-Rad, A. Islam, J.S. Jensen, A. Alnasser, Interaction of nanofillers in injection-molded graphene/carbon nanotube reinforced PA66 hybrid nanocomposites, J. Polym. Eng. 38 (2018) 971–981, https://doi.org/10.1515/polyeng-2018-0060.
[11] Y. Kim, J.S. Kim, S.-Y. Lee, R.L. Mahajan, Y.-T. Kim, Exploration of hybrid nanocarbon composite with polylactic acid for packaging applications, Int. J. Biol. Macromol. 144 (2020) 135–142, https://doi.org/10.1016/j.ijbiomac.2019.11.239.
[12] L. Li, L. Xu, W. Ding, H. Lu, C. Zhang, T. Liu, Molecular-engineered hybrid carbon nanofillers for thermoplastic polyurethane nanocomposites with high mechanical strength and toughness, Compos. B Eng. 177 (2019), 107381, https://doi.org/10.1016/j.compositesb.2019.107381.
[13] A. Rostami, M.I. Moosavi, High-performance thermoplastic polyurethane nanocomposites induced by hybrid application of functionalized graphene and carbon nanotubes, J. Appl. Polym. Sci. 137 (2020), 48520, https://doi.org/10.1002/app.48520.
[14] X. Su, R. Wang, X. Li, S. Araby, H.-C. Kuan, M. Naeem, J. Ma, A comparative study of polymer nanocomposites containing multi-walled carbon nanotubes and graphene nanoplatelets, Nano Mater. Sci. 4 (2022) 185–204, https://doi.org/10.1016/j.nanoms.2021.08.003.
[15] J. Li, P.-S. Wong, J.-K. Kim, Hybrid nanocomposites containing carbon nanotubes and graphite nanoplatelets, Mater. Sci. Eng. 483–484 (2008) 660–663, https://doi.org/10.1016/j.msea.2006.08.145.
[16] S. Kuester, N.R. Demarquette, J.C. Ferreira Jr., B.G. Soares, G.M.O. Barra, Hybrid nanocomposites of thermoplastic elastomer and carbon nanoadditives for electromagnetic shielding, Eur. Polym. J. 88 (2017) 328–339, https://doi.org/10.1016/j.eurpolymj.2017.01.023.
[17] Y.-j. Xiao, W.-y. Wang, X.-j. Chen, T. Lin, Y.-t. Zhang, J.-h. Yang, Y. Wang, Z.-w. Zhou, Hybrid network structure and thermal conductive properties in poly (vinylidene fluoride) composites based on carbon nanotubes and graphene

nanoplatelets, Composer Part A Appl. Sci. Manuf. 90 (2016) 614–625, https://doi.org/10.1016/j.compositesa.2016.08.029.
[18] K. Sa, P.C. Mahakul, S. Saha, P.N. Vishwakarma, K.K. Nanda, P. Mahanandia, Investigation of electrical, mechanical, and thermal properties of functionalized multiwalled carbon nanotubes-reduced graphene Oxide/PMMA hybrid nanocomposites, Polym. Eng. Sci. 59 (2019) 1075–1083, https://doi.org/10.1002/pen.25084.
[19] S. Dul, L.G. Ecco, A. Pegoretti, L. Fambri, Graphene/carbon nanotube hybrid nanocomposites: effect of compression molding and fused filament fabrication on properties, Polymers 12 (101) (2020), https://doi.org/10.3390/polym12010101.
[20] P. Russo, D. Acierno, G. Marletta, G.L. Destri, Tensile properties, thermal and morphological analysis of thermoplastic polyurethane films reinforced with multiwalled carbon nanotubes, Eur. Polym. J. 49 (2013) 3155–3164, https://doi.org/10.1016/j.eurpolymj.2013.07.021.
[21] A. Farzaneh, A. Rostami, H. Nazockdast, Thermoplastic polyurethane/multiwalled carbon nanotubes nanocomposites: effect of nanoparticle content, shear, and thermal processing, Polym. Compos. 42 (2021) 4804–4813, https://doi.org/10.1002/pc.26190.
[22] S. Kumar, T.K. Gupta, K.M. Varadarajan, Strong, stretchable and ultrasensitive MWCNT/TPU nanocomposites for piezoresistive strain sensing, Compos. B Eng. 177 (2019), 107285, https://doi.org/10.1016/j.compositesb.2019.107285.
[23] M. Albozahid, H.Z. Naji, Z.K. Alobad, A. Saiani, TPU nanocomposites tailored by graphene nanoplatelets: the investigation of dispersion approaches and annealing treatment on thermal and mechanical properties, Polym. Bull. 79 (2022) 8269–8307, https://doi.org/10.1007/s00289-021-03898-1.
[24] N. Aranburu, I. Otaegi, G. Guerrica-Echevarria, Using an ionic liquid to reduce the electrical percolation threshold in biobased thermoplastic polyurethane/graphene nanocomposites, Polymers 11 (2019) 435, https://doi.org/10.3390/polym11030435.
[25] H. Quan, B.-q. Zhang, Q. Zhao, R.K.K. Yuen, R.K.Y. Li, Facile preparation and thermal degradation studies of graphite nanoplatelets (GNPs) filled thermoplastic polyurethane (TPU) nanocomposites, Composer Part A Appl. Sci. Manuf. 40 (2009) 1506–1513, https://doi.org/10.1016/j.compositesa.2009.06.012.
[26] H. Liu, Y. Li, K. Dai, G. Zheng, C. Liu, C. Shen, X. Yan, J. Guo, Z. Guo, Electrically conductive thermoplastic elastomer nanocomposites at ultralow graphene loading levels for strain sensor applications, J. Mater. Chem. C 4 (2016) 157–166, https://doi.org/10.1039/C5TC02751A.
[27] H. Liu, J. Gao, W. Huang, K. Dai, G. Zheng, C. Liu, C. Shen, X. Yan, J. Guo, Z. Guo, Electrically conductive strain sensing polyurethane nanocomposites with synergistic carbon nanotubes and graphene bifillers, Nanoscale 8 (2016) 12977–12989, https://doi.org/10.1039/c6nr02216b.
[28] S. Roy, S.K. Srivastava, J. Pionteck, V. Mittal, Mechanically and thermally enhanced multiwalled carbon nanotube-graphene hybrid filled thermoplastic polyurethane nanocomposites, Macromol. Mater. Eng. 300 (2015) 346–357, https://doi.org/10.1002/mame.201400291.
[29] I. Otaegi, N. Aranburu, M. Iturrondobeitia, J. Ibarretxe, G. Guerrica-Echevarria, The effect of the preparation method and the Dispersion and Aspect Ratio of CNTs on the mechanical and electrical properties of bio-based polyamide-4,10/CNT nanocomposites, Polymers 11 (2019), https://doi.org/10.3390/polym11122059, 2059.
[30] T. McNally, P. Poetschke, in: Polymer-Carbon Nanotube Composites: Preparation, Properties and Applications, Woodhead Publishing, Cambridge, 2011, https://doi.org/10.1016/B978-1-84569-761-7.50028-9.
[31] F. Piana, J. Pionteck, Effect of the melt processing conditions on the conductive paths formation in thermoplastic polyurethane/expanded graphite (TPU/EG) composites, Compos. Sci. Technol. 80 (2013) 39–46, https://doi.org/10.1016/j.compscitech.2013.03.002.
[32] F. Askari, M. Barikani, M. Barmar, P. Shokrollahi, Polyurethane/amino-grafted multiwalled carbon nanotube nanocomposites: microstructure, thermal, mechanical, and rheological properties, J. Appl. Polym. Sci. 134 (2017), 44411, https://doi.org/10.1002/app.44411.
[33] A. Poosala, K. Hrimchum, D. Aussawasathien, D. Pentrakoon, The effect of oxygen-plasma treated graphene nanoplatelets upon the properties of multiwalled carbon nanotube and polycarbonate hybrid nanocomposites used for electrostatic dissipative applications, J. Nanomater. 470297 (2015) 2015, https://doi.org/10.1155/2015/470297.
[34] Technical datasheet, Cheaptubes MWCNT 20-30 nm, Available on: https://www.cheaptubes.com/product/multi-walled-carbon-nanotubes-20-30nm. (Accessed 23 March 2023).
[35] B.N. Duc, Y. Son, Effect of aspect ratio, bulk density, and production date of multi-walled carbon nanotubes on the electrical conductivity of polypropylene and polycarbonate/multi-walled carbon nanotube nanocomposites, J. Compos. Mater. 56 (2022) 3529–3539, https://doi.org/10.1177/00219983221113384.
[36] I.M. Inuwa, R. Arjmandi, A.N. Ibrahim, M.K.M. Haafiz, S.L. Wong, K. Majeed, A. Hassan, Enhanced mechanical and thermal properties of hybrid graphene nanoplatelets/multiwall carbon nanotubes reinforced polyethylene terephthalate nanocomposites, Fibers Polym. 17 (2016) 1657–1666, https://doi.org/10.1007/s12221-016-6238-9.
[37] D. Stauffer, A. Aharony, in: Introduction to Percolation Theory, Taylor & Francis, London, 1994, https://doi.org/10.1201/9781315274386.
[38] S. Kumar, L.L. Sun, S. Caceres, B. Li, W. Wood, A. Perugini, R.G. Maguire, W. H. Zhong, Dynamic synergy of graphitic nanoplatelets and multi-walled carbon nanotubes in polyetherimide nanocomposites, Nanotechnology 21 (2010), 105702, https://doi.org/10.1088/0957-4484/21/10/105702.
[39] M.H. Al-Saleh, Electrical and mechanical properties of graphene/carbon nanotube hybrid nanocomposites, Synth. Met. 209 (2015) 41–46, https://doi.org/10.1016/j.synthmet.2015.06.023.
[40] R. Kotsilkova, I. Petrova-Doycheva, D. Menseidov, E. Ivanov, A. Paddubskaya, P. Kuzhir, Exploring thermal annealing and graphene-carbon nanotube additives to enhance crystallinity, thermal, electrical and tensile properties of aged poly(lactic) acid-based filament for 3D printing, Compos. Sci. Technol. 181 (2019), 107712, https://doi.org/10.1016/j.compscitech.2019.107712.
[41] P. Pokharel, D. Xiao, F. Erogbogbo, O. Keles, D.S. Lee, A hierarchical approach for creating electrically conductive network structure in polyurethane nanocomposites using a hybrid of graphene nanoplatelets, carbon black and multi-walled carbon nanotubes, Compos. B Eng. 161 (2019) 169–182, https://doi.org/10.1016/j.compositesb.2018.10.057.
[42] C. Garzon, H. Palza, Electrical behavior of polypropylene composites melt mixed with carbon-based particles: effect of the kind of particle and annealing process, Compos. Sci. Technol. 99 (2014) 117–123, https://doi.org/10.1016/j.compscitech.2014.05.018.
[43] N. Aranburu, J.I. Eguiazabal, Electrically conductive multi-walled carbon nanotube-reinforced amorphous polyamide nanocomposites, Polym. Compos. 35 (2014) 587–595, https://doi.org/10.1002/pc.22699.
[44] C. Salom, M.G. Prolongo, A. Toribio, A.J. Martínez-Martínez, I. Aguirre de Cárcer, S.G. Prolongo, Mechanical properties and adhesive behavior of epoxy-graphene nanocomposites, Int. J. Adhesion Adhes. 84 (2018) 119–125, https://doi.org/10.1016/j.ijadhadh.2017.12.004.
[45] P. Jojibabu, M. Jagannatham, P. Haridoss, G.D.J. Ram, A.P. Deshpande, S. R. Bakshi, Effect of different carbon nano-fillers on rheological properties and lap shear strength of epoxy adhesive joints, Composer Part A Appl. Sci. Manuf. 82 (2016) 53–64, https://doi.org/10.1016/j.compositesa.2015.12.003.
[46] R. Mactabi, I.D. Rosca, S.V. Hoa, Monitoring the integrity of adhesive joints during fatigue loading using carbon nanotubes, Compos. Sci. Technol. 78 (2013) 1–9, https://doi.org/10.1016/j.compscitech.2013.01.020.
[47] S. Han, Q. Meng, X. Pan, T. Liu, S. Zhang, Y. Wang, S. Haridy, S. Araby, Synergistic effect of graphene and carbon nanotube on lap shear strength and electrical conductivity of epoxy adhesives, J. Appl. Polym. Sci. 136 (2019), 48056, https://doi.org/10.1002/app.48056.